Phonons and fundamental gap in ZnSe: Effects of the isotopic composition

A. Göbel, T. Ruf, J. M. Zhang,* R. Lauck, and M. Cardona
Max-Planck-Institut für Festkörperforschung, Heisenbergstrasse 1, D-70569 Stuttgart, Germany
(Received 9 September 1998)

We have investigated the effects of isotopic composition on the phonon frequencies and linewidths as well as the fundamental gap of ZnSe on a series of samples made from the stable isotopes ^{64}Zn, ^{68}Zn, ^{76}Se, and ^{80}Se. Besides four nearly isotopically pure samples, we have measured natural ZnSe, which is highly isotopically disordered. In addition, we have investigated samples with monoisotopic cation or anion sublattices for which the anion or cation sublattice, respectively, consists of an artificial mixture of isotopes. Using Raman spectroscopy, we find a TO(Γ) linewidth of $\sim$0.4 cm^{-1} for nominally isotopically pure samples at low temperatures, as compared to 1.75(1) cm^{-1} in natural ZnSe. In samples with only cation or anion disorder, the linewidths amount to 1.16(6) cm^{-1} (^{dis}Zn^{80}Se) and 0.84(3) cm^{-1} (^{68}Zn^{dis}Se). This strong isotope-disorder-induced broadening of the TO(Γ) phonon can be attributed to a large one-phonon density of states in this energy range. With linear optical spectroscopy (luminescence), we find, also at low temperature, that the fundamental gap of ZnSe increases by 214(30) μeV/amu when increasing the Zn mass. It increases by 216(30) μeV/amu when increasing the Se mass. A two-harmonic-oscillator model for the temperature dependence of the gap yields values for its mass dependence that are in qualitative agreement with this observation. [S0163-1829(99)09803-3]

I. INTRODUCTION

Isotope substitution is a well-defined and easily controlable method to investigate intrinsic renormalization mechanisms of elementary excitations in semiconductors. Results gained mostly from elemental semiconductors have been reviewed in several publications.[1–4] Recently, we have turned our attention to binary compound semiconductors, for which the elements on the cation or anion sublattices can be substituted independently. The degree of sophistication achievable in these studies often depends on the fundamental properties of the material in question.

First of all, phonon frequencies are directly affected by changes of the average mass of the whole crystal or its sublattices (virtual crystal approximation), even when we look upon them as noninteracting particles, i.e., as harmonic oscillators. In elemental semiconductors those frequencies depend on the inverse of the square root of the mass [$\omega(\mathbf{q}) \sim m^{-1/2}$] for all wave vectors $\mathbf{q}$, while the mass dependence becomes $\mathbf{q}$ dependent in the case of compounds. The direct influence of the isotope mass on the frequencies of coupled phonon modes has been used to determine their eigenvectors, e.g., in CdS,[5] GaN,[6] and SiC.[7] Secondly, the mean square vibrational amplitudes $\langle u^2 \rangle$ of phonons depend on the isotope masses only at low temperature, while they are determined by the temperature T only, once T becomes larger than the Debye temperature.[1]

A refinement of these effects must take place when taking interactions among phonons into account. These interactions lead to finite phonon lifetimes and additional frequency renormalizations. The underlying processes can be divided into two classes: (i) *anharmonic interactions* in which, e.g., a zone center phonon decays into two phonons (or more) with wave-vector and energy conservation, and (ii) *elastic scattering* in which a phonon scatters into phonons of similar energies but different wave vectors $\mathbf{q}$. While the former processes arise from cubic and quartic terms in the expansion of the lattice potential, the latter are due to the relaxed wave-vector conservation rule in samples that are isotopically disordered and thus not strictly translationally invariant. Since the vast majority of semiconductors derive from elements having more than one stable isotope, it is clear that both processes are present most of the time. Unfortunately, their absolute sizes and relative importance cannot be predicted easily. However, isotope enrichment allows one to suppress the elastic scattering induced by isotope disorder. Systematic substitution of pure isotopes in CuCl has been used to selectively tune the efficiency of anharmonic decay channels of the zone center TO phonon independent of isotope scattering and thus the direct analysis of the effects of anharmonic renormalization has been possible.[8] In contrast, the anharmonic phonon-phonon interaction cannot be suppressed, so that isotope-disorder-induced effects can only be studied against a background contribution from anharmonic processes. However, if one assumes that the two processes are independent of each other one can measure the disorder-induced renormalization by comparison of phonon energies and linewidths of istopically pure samples with those gained from disordered ones. This has been done for optical phonons in germanium throughout the Brillouin zone (BZ) by means of inelastic neutron scattering[9] and for the zone center phonons of Ge,[10] Si,[11] and α-Sn (Ref. 12) as well as GaAs (Ref. 11) by means of Raman scattering.

In another step of refinement, the renormalization of the fundamental electronic gap by *electron-phonon interaction* also depends on the isotope mass. Although the electronic properties of different isotopes of a given atom are, to a very good approximation, the same, isotope substitution in a crystal modifies the phonon spectrum[13] which, in turn, modifies the electron energy bands through electron-phonon interaction. Measuring the energy gaps in samples with different isotopic composition then yields the difference in the

TABLE I. Reduced mass μ, average sublattice mass $\overline{m}_\kappa$, and sublattice mass variance parameters $g(\kappa)$ for the ZnSe samples investigated. Errors in g are smaller than 10^{-5}.

	$^{64}Zn^{76}Se$	$^{64}Zn^{80}Se$	$^{nat}Zn^{nat}Se$	$^{68}Zn^{76}Se$	$^{dis}Zn^{80}Se$	$^{68}Zn^{dis}Se$	$^{68}Zn^{80}Se$
μ [amu]	34.73(1)	35.52(1)	35.77(1)	35.85(1)	36.13(1)	36.29(1)	36.70(1)
$\overline{m}_{Zn}$ [amu]	63.945	63.945	65.396	68.865	65.950	67.865	67.865
$\overline{m}_{Se}$ [amu]	76.010	79.900	78.957	76.010	79.900	77.990	79.900
$g(Zn)[10^{-4}]$	0.12	0.12	5.95	0.42	9.28	0.42	0.42
$g(Se)[10^{-4}]$	0.56	0.22	4.63	0.56	0.22	6.67	0.22

changes of the valence- and conduction-band renormalization. CuCl is a textbook example since its phonon spectrum can be approximated by an acoustic copperlike and an optic chlorinelike harmonic oscillator. As a result, the effects of cation and anion substitution on the band-gap renormalization can be disentangled and the observed anomalous increase of the band gap with increasing temperature can be quantitatively understood.[14,15] Other experimental examples are the changes of band gaps of Ge,[16,17] GaAs,[13] and CdS (Ref. 18) upon isotope substitution.

In a way similar to the thermal expansion, one finds that the dependence of the lattice constant on the isotope masses arises from an *integral* over all occupied phonon states weighted by their Grüneisen parameters.[13,19–21] This isotopic lattice expansion cannot be suppressed (since it arises from anharmonic effects and is a form of a macroscopic quantum effect). It also gives additional contributions to the changes in gap energies. However, these contributions are (usually) smaller than those arising from the direct electron-phonon interaction.[13,17,21] We note also that the thermal conductivity, i.e., another macroscopic quantity, is strongly affected by the isotope-disorder-induced scattering of phonons. This effect has been studied recently for Ge and Si.[22]

In this paper, we deal with a number of the effects described above that we have identified in ZnSe. One issue of particular interest is the lifetime of the transverse optic phonon at the BZ center, which in the case of natural ZnSe could previously not be attributed to anharmonic decay only.[23,24] We have measured transverse (TO) and longitudinal (LO) optical phonons by means of Raman scattering at low temperatures (2 K) on nominally isotopically pure and on isotopically disordered samples. For the latter samples we find additional contributions to the frequency and linewidth of the TO(Γ) phonon which we discuss in the framework of mass-disorder-induced scattering. For the LO(Γ) phonons we neither find a significant isotope disorder contribution to their energy nor can we discern a disorder-induced broadening from other contributions to the linewidth. The influence of potential contributions from plasmon-phonon coupling and anharmonic interactions is discussed.

We also use *isotope substitution* to tune the phonon frequencies in our samples and measure the corresponding changes in the band gap as observed in their luminescence spectra at 2 K. For cation and anion substitution we find the usual[1,13,18] gap *increase* with *increasing* mass. This type of behavior has been also observed in elemental and compound semiconductors. We describe the band-gap renormalization as being caused by two effective phonon oscillators. A fit of the temperature dependence of the fundamental gap[25] yields values that are in qualitative agreement with the experimentally determined mass dependences.

The paper is organized as follows: In Sec. II we present the samples and experimental detail. In Sec. III we show the data obtained from Raman scattering and luminescence measurements. We discuss our results for the TO(Γ) phonons in Sec. IV A and those for the LO(Γ) in Sec. IV B. The mass and temperature dependence of the fundamental gap is dealt with in terms of a two-oscillator model in Sec. IV C. The conclusions are drawn in Sec. V.

II. SAMPLES AND EXPERIMENTAL DETAILS

Natural zinc selenide is an isotopically disordered material, since natural Zn contains five isotopes (^{64}Zn:48.6%, ^{66}Zn:27.9%, ^{67}Zn:4.1%, ^{68}Zn:18.8%, ^{70}Zn:0.6%) and natural Se contains six isotopes (^{74}Se:0.9%, ^{76}Se:9.4%, ^{77}Se:7.6%, ^{78}Se:23.8%, ^{80}Se:49.6%, ^{82}Se:8.7%).[26] The mass differences between the lightest and heaviest isotopes amount to about 10% in both cases. A measure for the mass disorder in a crystal can be obtained from the mass variance of each sublattice,[27]

$$g(\kappa)=\sum_i c_i\left(\frac{m_i-\overline{m}}{\overline{m}}\right)^2, \tag{1}$$

where c_i is the concentration of the respective isotope, m_i its mass, and $\overline{m}$ is the average mass of the particular composition of the element κ. We have investigated natural ZnSe and six ZnSe samples of artificial isotopic composition. The elements used to grow our samples were highly isotopically enriched, although not isotopically pure, i.e., some of the source materials contained two other isotopes, up to 1.5% of each. We have determined their isotopic composition by means of mass spectroscopy to within 1%. The isotopic composition of the ^{dis}Zn^{80}Se sample (nominally $^{64}Zn_{0.5}{}^{68}Zn_{0.5}{}^{80}$Se) was determined as ^{64}Zn:49.1%, ^{66}Zn:1.0%, ^{67}Zn:1.5%, ^{68}Zn:47.3%, ^{70}Zn:1.1%, ^{80}Se: $\geqslant$98.5%, that of ^{68}Zn^{dis}Se (nominally $^{68}Zn^{76}Se_{0.5}{}^{80}Se_{0.5}$) as ^{74}Se:0.4%, ^{76}Se:47.0%, ^{77}Se:0.4%, ^{78}Se:1.3%, ^{80}Se:50.2%, ^{82}Se:0.7%, and ^{68}Zn:$\geqslant$98%. The sublattice mass variances, the reduced masses μ ($\mu^{-1}=m_{Zn}^{-1}+m_{Se}^{-1}$), and the average sublattice masses of the samples are listed in Table I. In some cases, the samples are large needles ($1\times2\times10$ mm^3) while other samples are an agglomerate of small micrometer- to millimeter-size grains. Whether these grains are single crystals or strongly twinned could not be determined. However, in all cases we have only detected LO

and TO Raman signals as expected for a zinc-blende compound. The crystal growth has been described elsewhere.[28] To check whether the crystal growth procedure and the sample shape have an influence on the phonon energies or linewidths, we have compared data obtained from several self-grown natural ZnSe crystals to those from a commercially available single crystal. We did not find any significant deviations.

The Raman spectra were excited with 5 mW of the 488-nm argon laser line. Other laser lines (458 nm, 476 nm) were used to check for line-shape distortions or shifts due to resonance effects. The spectra were calibrated with respect to the 4921.931-Å helium emission line. To determine the phonon energies, the spectral slitwidth was set to 20 μm; for the linewidths measurements, we used slits of 15 μm width. These values correspond to a spectral resolution of 0.31 cm^{-1} and 0.24 cm^{-1}, respectively. By measurements of very narrow plasma lines and of the laser line, we have checked that the instrumental resolution, at the slit widths used, is well approximated by a Gaussian line shape. Consequently, we have fitted all phonon spectra with a Voigt profile[29] in which the Gaussian widths were set to the above values. For the luminescence spectra, we excited the samples with the 413-nm line of a krypton ion laser. The laser power was kept below 0.2 mW, and the spectra were calibrated against the 4425.189-Å krypton emission line. In both experiments, we used single-photon counting techniques, a backscattering geometry and dispersed the light with a SPEX 1404 double monochromator ($f=0.85$ m). The samples were cooled to 1.8–2 K by immersion in superfluid helium. Special care was taken to avoid sample heating.

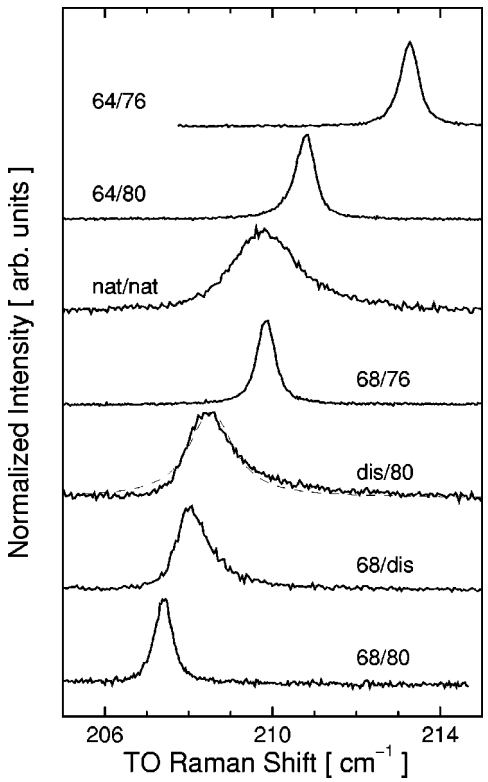

FIG. 1. Raman spectra of the TO phonons of isotopically modified ZnSe taken at 2 K. The ZnSe compositions are indicated next to each spectrum. All spectra are normalized to the same height. The integration times were the same for all spectra, a fact that accounts for the differing signal-to-noise ratios. In addition, we show the fit of a Voigt profile to the asymmetric spectra of $^{dis}Zn^{80}Se$ as a dashed line.

III. RESULTS

We have investigated seven ZnSe samples that cover a wide range of reduced and average zinc and selenium masses. Four samples ($^{64}Zn^{76}Se$, $^{64}Zn^{80}Se$, $^{68}Zn^{76}Se$, and $^{68}Zn^{80}Se$) are nearly isotopically pure ($g \leqslant 10^{-4}$). The natural ZnSe sample exhibits mass disorder on both sublattices. Two samples ($^{dis}Zn^{80}Se$, $^{68}Zn^{dis}Se$) exhibit isotope disorder on their cation or anion sublattices only (compare Table I). The error bars for the phonon frequencies and linewidths indicated in the figures are the mean square deviation of at least three spectra obtained on different spots of each sample.

A. TO(Γ) phonons

In Fig. 1, we show the Raman spectra of the transverse optical phonon in ZnSe for several isotopic compositions. The reduced vibrational mass decreases from the bottom to the top spectrum. The isotopically pure samples $^{64}Zn^{76}Se$, $^{64}Zn^{80}Se$, $^{68}Zn^{76}Se$, and $^{64}Zn^{80}Se$ show very narrow and symmetric line shapes. In contrast, the Raman spectra of the isotopically disordered samples $^{nat}Zn^{nat}Se$, $^{dis}Zn^{80}Se$, and $^{68}Zn^{dis}Se$ are substantially broadened and asymmetric, with a shoulder towards higher energies. It is clear from Fig. 1 that one has to be careful when fitting the asymmetric TO(Γ) line shapes in particular for the $^{dis}Zn^{80}Se$ and $^{68}Zn^{dis}Se$ samples. Lacking an analytic expression for the disorder-broadened phonon line shape, we have fitted symmetric Voigt profiles to the spectra, and assured that the fits have similar heights and describe the linewidths well. As an example, we show a fit to the TO(Γ) spectrum of $^{dis}Zn^{80}Se$ as the dashed line. The nominal phonon frequencies and widths were taken from these fits. It should be noted that one can use other procedures to obtain a measure of the disorder-induced shifts and broadenings, e.g., a weighted average and the variance of the phonon frequency, respectively.[9] As a result the actual values might change slightly.

The TO(Γ) phonon frequencies are plotted in Fig. 2 as a function of the reduced masses of the samples. For the isotopically pure samples, we expect these energies to depend on the reduced mass only (except for the changes of the anharmonic renormalization upon isotope substitution that are too small to be extracted from our data). Consequently, we have fitted them to a $\mu^{-1/2}$ curve, shown by the solid line in Fig. 2. The quality of this fit is excellent. The TO(Γ) energies of the isotopically disordered samples deviate from the $\mu^{-1/2}$ behavior. They show additional shifts of $-0.28(5)cm^{-1}$ ($^{nat}Zn^{nat}Se$), $-0.50(5)cm^{-1}$ ($^{dis}Zn^{80}Se$), and $-0.42(8)cm^{-1}$ ($^{68}Zn^{dis}Se$) towards lower energies. We attribute these shifts to a disorder-induced self-energy arising from the scattering of the zone center phonon into phonons with similar frequencies but with different wave vectors **q**. These disorder effects become even more pronounced when we consider the linewidths.

In Fig. 3, we show the TO(Γ) widths (FWHM) of the isotopically pure samples by open circles. From the fits with

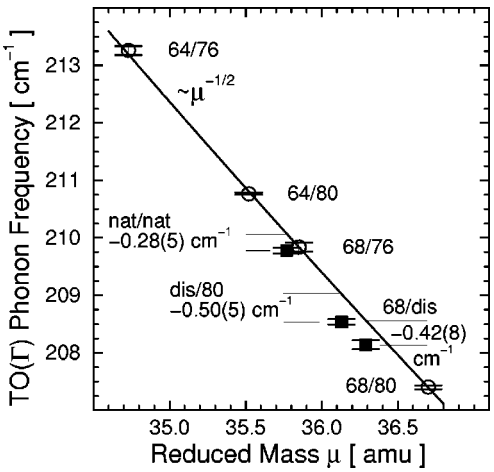

FIG. 2. Transverse-optical-phonon frequencies at the center of the BZ for isotopically modified ZnSe samples at 2 K as a function of the reduced mass. The open circles correspond to isotopically pure samples, the filled squares to isotopically disordered samples. The line represents the predictions of the harmonic approximations. Some points fall below the line because of frequency renormalization by isotope disorder.

Voigt profiles, we find widths of $0.40(3)\mathrm{cm}^{-1}$. As a guide to the eye we have fitted a μ^{-1} dependence to these linewidths, which is shown as the solid line. The linewidths of the isotopically disordered samples (filled squares) are up to a factor of 4 (!) larger: $1.75(1)\mathrm{cm}^{-1}$ ($^{\mathrm{nat}}\mathrm{Zn}^{\mathrm{nat}}\mathrm{Se}$), $1.16(6)\mathrm{cm}^{-1}$ ($^{\mathrm{dis}}\mathrm{Zn}^{80}\mathrm{Se}$), and $0.84(3)\mathrm{cm}^{-1}$ ($^{68}\mathrm{Zn}^{\mathrm{dis}}\mathrm{Se}$). We attribute the additional contribution to isotope-disorder-induced scattering that will be discussed in Sec. IV A.

B. LO(Γ) phonons

In Fig. 4, we show the LO-phonon Raman spectra of our ZnSe samples obtained at 2 K. The spectra for the isotopically pure and disordered samples are symmetric except for those of $^{64}\mathrm{Zn}^{76}\mathrm{Se}$ and $^{64}\mathrm{Zn}^{80}\mathrm{Se}$. The corresponding LO(Γ) phonon frequencies are shown in Fig. 5 as a function of the reduced mass. We cannot discern any systematic deviation of the isotopically disordered samples from the reduced mass dependence (the solid line was fitted to the data of the isotopically pure samples only), although one could, in principle, expect an additional shift towards higher energies.[10,12] The LO(Γ)-phonon linewidths [full width at half maximum (FWHM)] vary between 1.1 and 2.0 cm^{-1} among the samples, with natural ZnSe, having the largest mass variance, exhibiting the smallest linewidth. We note that our

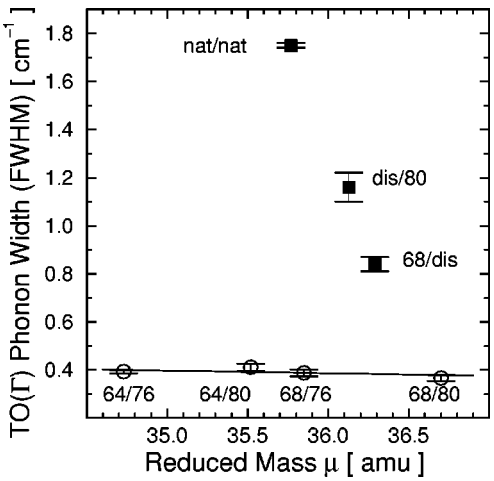

FIG. 3. Transverse-optical-phonon linewidths (FWHM) at the center of the BZ for isotopically modified ZnSe samples at 2 K as a function of the reduced mass. The open circles correspond to isotopically pure samples, the filled squares to isotopically disordered samples.

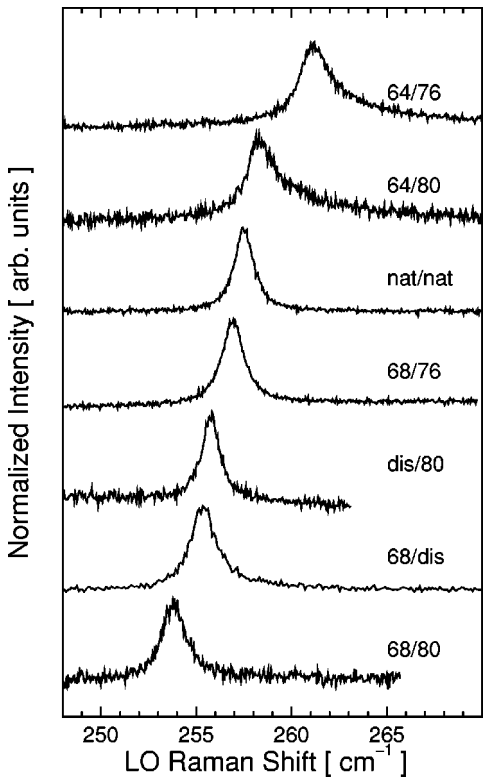

FIG. 4. Raman spectra of LO phonons from samples of isotopically modified ZnSe taken at 2 K.

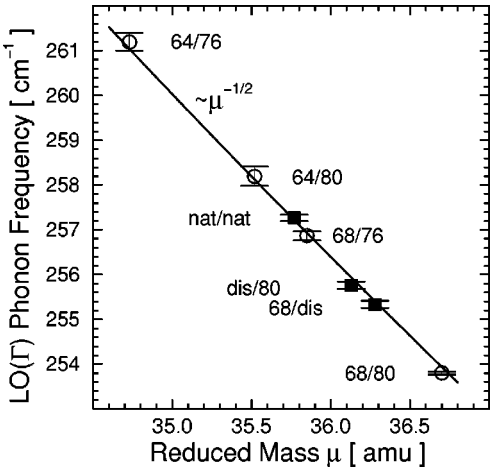

FIG. 5. Longitudinal-optical-phonon frequencies at the center of the BZ for isotopically modified ZnSe samples at 2 K as a function of the reduced mass. The open circles correspond to isotopically pure samples, the filled squares to isotopically disordered samples. For the fit to $\mu^{-1/2}$, only the values from isotopically pure samples were used.

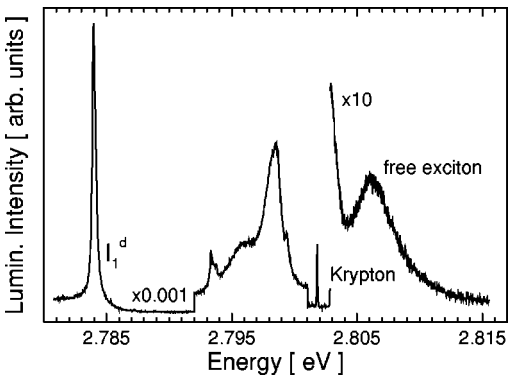

FIG. 6. Luminescence spectrum of $^{dis}Zn^{80}Se$ at 2 K. The emission peaks from free excitons and acceptor-bound excitons, I_1^d, are correspondingly labeled.

natural samples yield TO(Γ) and LO(Γ) widths that are up to 50% smaller than those reported by Anand *et al.*[24]

C. Luminescence

We show in Fig. 6 the luminescence spectrum of the $^{dis}Zn^{80}Se$ sample at 2 K in order to explain the various features observed. The 4425.189-Å (2801.815 meV) krypton emission line was used to calibrate the spectrum. The free-exciton transition could not be observed in all samples. Furthermore, it is rather broad and it appears to be superimposed on a strongly varying background that is not very well defined. Therefore, the mass dependence of the band gap could not be inferred from the free-exciton luminescence. Instead, we have turned to the considerably narrower and more intense I_1^d transition, which is commonly associated with an acceptor-bound exciton.[30] Neglecting the isotope mass dependence of the exciton binding energy and of the acceptor binding energy, which are expected to be very small, we identify the changes of the I_1^d transition upon isotope substitution with changes of the band gap renormalization itself. In Fig. 7, we show the I_1^d transitions obtained from $^{64}Zn^{76}Se$, $^{64}Zn^{80}Se$, $^{dis}Zn^{80}Se$, and $^{68}Zn^{80}Se$. These lines are narrow in comparison with the isotope effect and are thus well suited to

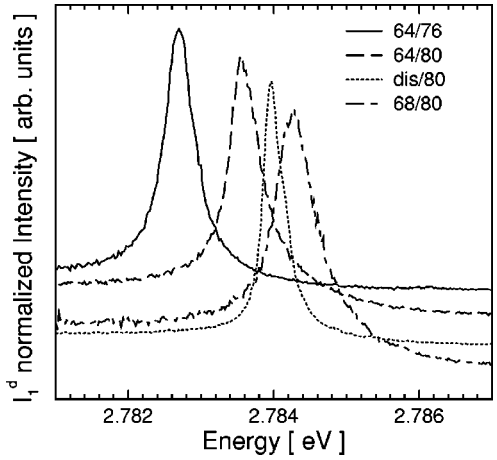

FIG. 7. Luminescence spectra of acceptor bound excitons, I_1^d, in ZnSe obtained from samples with different isotopic composition at 2 K. The transition energy increases with an increase in both the Zn and Se masses.

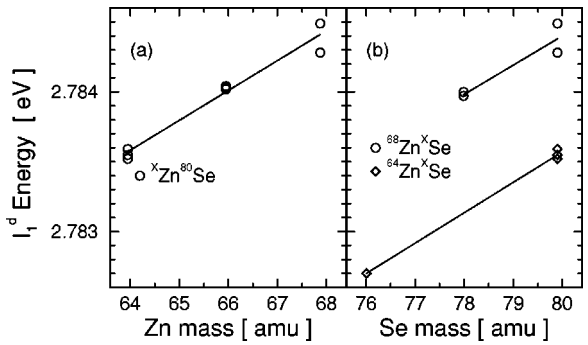

FIG. 8. Transition energies of the acceptor-bound exciton, I_1^d, in ZnSe samples of different isotopic composition. (a) and (b) show the mass dependence for cation and anion substitution, respectively. The solid lines are linear regression fits to the data.

determine the gap shift, in spite of some variations in their linewidths, shape, and background. The I_1^d energies are plotted as a function of the cation and anion mass in Figs. 8(a) and 8(b), respectively. In both cases, we find a band-gap increase with increasing masses and obtain $\partial E_0/\partial m_{Zn} = +214(30)\,\mu$eV/amu and $\partial E_0/\partial m_{Se} = +216(30)\,\mu$eV/amu from linear regressions shown by the solid lines.

IV. DISCUSSION

A. Isotope disorder

We assume that all Zn and Se atoms are located on their ideal sites. Even in the case of such a *perfect* crystal, mass fluctuations occur on the sublattices, i.e., the isotopes are randomly distributed throughout the lattice according to their relative abundances. Therefore, the translational invariance of the crystal is (weakly) broken, and, consequently, crystal momentum does not need to be strictly conserved, so that elastic scattering of phonons becomes allowed. Tamura has treated the case of isotope disorder in monoatomic lattices for the case of germanium[31] and calculated the lifetimes of acoustic phonons in the framework of a mass perturbation of the harmonic lattice dynamical Hamiltonian. He has subsequently extended this approach to zinc-blende GaAs and InSb.[27] Here, we only summarize the main results: The isotope-disorder-induced scattering rate τ_{iso}^{-1} of the phonon labeled by the branch index j and the wave vector $\mathbf{q}$, with energy $\omega_j(\mathbf{q})$ is given by

$$\tau_{iso}^{-1}(j\mathbf{q};\omega) = \frac{\pi}{6N}\omega_j^2(\mathbf{q})\sum_{\kappa} g(\kappa)|\mathbf{e}(\kappa|j\mathbf{q})|^2 \times \sum_{j',\mathbf{q}'} |\mathbf{e}(\kappa|j'\mathbf{q}')|^2 \delta[\omega-\omega_{j'}(\mathbf{q}')] \tag{2}$$

$$= \frac{\pi}{6}\omega_j^2(\mathbf{q})\sum_{\kappa} g(\kappa)|\mathbf{e}(\kappa|j\mathbf{q})|^2 \rho_\kappa(\omega), \tag{3}$$

for the case of zinc-blende compounds. The orthonormal eigenvectors of the sublattice κ of the considered phonon $j\mathbf{q}$ and those of the phonons $j'\mathbf{q}'$ it is scattered into are denoted by $\mathbf{e}(\kappa|j\mathbf{q})$ and $\mathbf{e}(\kappa|j'\mathbf{q}')$, respectively. The real-space displacements are given by the usual expression $\mathbf{u}(\kappa|j\mathbf{q}) = m_\kappa^{-1/2}\mathbf{e}(\kappa|j\mathbf{q})$. The mass variance for each sublattice is

denoted by $g(\kappa)$ and the δ function ensures energy conservation. Thus the scattering rate τ_{iso}^{-1} is determined by the squared eigenvectors of the atomic vibration associated with the initial state multiplied by the projected density of states (DOS) $\rho_\kappa(\omega)$. The projected one-phonon density of final states $\rho_\kappa(\omega)$ is obtained when weighing each state by the square of the respective sublattice eigenvector $|\mathbf{e}(\kappa|j\mathbf{q})|^2$. The total (i.e., unweighted) DOS is normalized to 6.

We associate the scattering rate τ_{iso}^{-1} with the imaginary part Γ_{iso} of the disorder-induced self-energy $\Pi_{iso}(j\mathbf{q};\omega) = \Delta_{iso}(j\mathbf{q};\omega) + i\frac{1}{2}\Gamma_{iso}(j\mathbf{q};\omega)$ of the phonon $j\mathbf{q}$. The real part Δ_{iso} can be obtained through a Kramers-Kronig transformation of Γ_{iso},

$$\Delta(j\mathbf{q};\omega) = -\frac{\pi}{6}\omega_j^2(\mathbf{q})\sum_\kappa g(\kappa)|\mathbf{e}(\kappa|j\mathbf{q})|^2 \times \frac{1}{\pi} P\int_0^\infty \frac{\omega'\rho_\kappa(\omega')}{\omega'^2-\omega^2}d\omega'. \quad (4)$$

Finally, we obtain the line shape from the spectral density function,

$$I(j\mathbf{q};\omega) \propto \frac{\Gamma_{iso}(j\mathbf{q};\omega)/2}{[\omega-\omega_j(\mathbf{q})-\Delta_{iso}(j\mathbf{q};\omega)]^2+\Gamma_{iso}^2(j\mathbf{q};\omega)/4}, \quad (5)$$

where $\Gamma_{iso}(j\mathbf{q};\omega)$ corresponds to the FWHM.

Figure 9(a) shows the projected one-phonon density of final states $\rho_{Se}(\omega)$ and $\rho_{Zn}(\omega)$ for $^{nat}Zn^{nat}Se$. Here, we have used the rigid-ion model[32] (RIM) and the parameters of Ref. 33 to describe the lattice dynamics of ZnSe. From these two lines, it is obvious that the independent adjustment of isotope disorder on each sublattice, in principle, opens new opportunities to investigate isotope-disorder-induced scattering: while the peaks at 213 cm^{-1} have very similar heights in both $\rho_\kappa(\omega)$, the partial densities of states differ strongly for all larger frequencies. Therefore, the shape of $\Gamma_{iso}(\omega)$ can be altered by the experimentalist when carefully adjusting the mass variance parameters $g(\kappa)$ on the cation and anion sublattices.

Figure 9(b) shows the disorder-induced broadening Γ_{iso} (FWHM) and the shift Δ_{iso} calculated for $^{nat}Zn^{nat}Se$. In order to avoid unphysically sharp peaks, Γ_{iso} was calculated from the $\rho_\kappa(\omega)$'s after they were convoluted with a Lorentzian of 0.4 cm^{-1} width (FWHM), corresponding to the anharmonic broadening. Simulated spectra are shown in Fig. 9(c) for three different frequencies $\omega_{TO}(\mathbf{q}=0)$. Obviously, the line shape is very sensitive to the location of $\omega_{TO}(\mathbf{q}=0)$ with respect to the sharp onset of Γ_{iso} in Fig. 9(b). We note that using the RIM for the lattice dynamics, the unrenormalized zone center frequencies $\omega_{TO}(\mathbf{q}=0)$ and the one-phonon density of states do not quantitatively reproduce the line shapes and trends we have observed. This is not surprising, since the range of a large DOS, i.e., large Γ_{iso} in Fig. 9(b) is very narrow (3–4 cm^{-1}), and its detailed shape is not known very precisely. The accuracy of the neutron data is at best ± 2 cm^{-1} and the RIM was fitted to the data obtained from acoustic branches *at room temperature*. Only three data points in optic branches were available for the fits.[33–36]

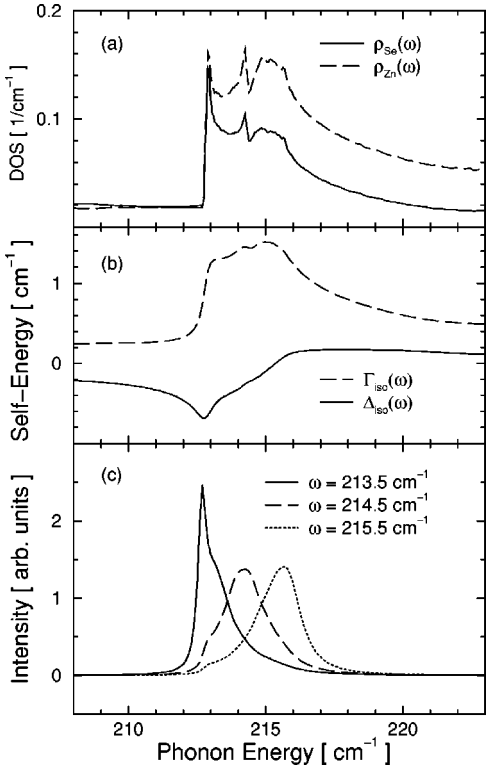

FIG. 9. (a) The weighted one-phonon density of states of each of the two sublattices obtained from the RIM with the parameters of Ref. 33. (b) The real and imaginary parts of the disorder-induced self-energy are represented by the dashed and the solid line, respectively, for the case of $^{nat}Zn^{nat}Se$. (c) Simulated spectra for several unrenormalized TO(Γ) frequencies $\omega_{TO}(\mathbf{q}=0)$.

Nevertheless, from the above treatment, we can extract the following qualitative conclusions: (i) In the case of $^{nat}Zn^{nat}Se$, the calculated broadening Γ_{iso} of about 1.4 cm^{-1} is in good agreement with the experiment ($\sim$1.4 cm^{-1}), and the line shape obtained for $\omega_{TO}(\mathbf{q}=0)=214.5$ cm^{-1} is similar to the experimental observation. The RIM yields 213 cm^{-1} for the unrenormalized TO(Γ) frequency. Since the use of this value in Eq. (5) does not yield a symmetric line shape, we conclude that the RIM does not reproduce the exact relative positions of $\omega_{TO}(\mathbf{q}=0)$ with respect to the branches which yield the large Γ_{iso}. (ii) The calculated negative line shifts of up to -0.5 cm^{-1}, when compared to the reduced-mass behavior observed in the isotopically pure samples, are approximately given by Δ_{iso} [see Fig. 9(a)] and are compatible with the experiment. We note that the sign of this effect is the opposite of that found for group-IV materials.[10,12] This can be understood in simple terms from the DOS, which in disorder-induced scattering repels the bare phonon. Therefore, the BZ center phonon in group-IV materials is shifted to higher frequencies, while the frequency of TO(Γ) in ZnSe is reduced. (iii) The steep low-energy flank of the DOS together with a zone center frequency $\omega_{TO}(\mathbf{q}=0)$, which is only slightly larger than the position of the flank (i.e., $\leqslant 1$ cm^{-1}), can lead to asymmetric line shapes similar to those observed for $^{68}Zn^{dis}Se$ and $^{dis}Zn^{80}Se$. An example for the resulting line shape is shown in Fig. 9(c) for $\omega_{TO}(\mathbf{q}=0)=213.5$ cm^{-1}. (iv) Along these lines, we obtain broadenings of 0.4 and 1.4 cm^{-1} for the $^{68}Zn^{dis}Se$ and $^{dis}Zn^{80}Se$ samples, respectively. The latter

value is somewhat larger than our experimental observation; we interpret this as hint that the eigenvectors and dispersion of the flat TO branches are not quantitatively well described by the RIM. (v) The disorder-induced self-energy Δ_{iso} which we calculate for LO(Γ) is on the order of $+0.2$ cm^{-1}, while the calculated broadening Γ_{iso} is on the order of 0.01 cm^{-1}. These small values are compatible with our experimental results from which we were not able to discern disorder-induced effects on the LO phonons. It should be noted that the LO(Γ) broadening calculated within this framework does not vanish only because we have convoluted the $\rho_\kappa(\omega)$'s with an anharmonic broadening. A similar convolution was employed to explain the small but finite disorder-induced broadening in Ge (Ref. 10) and Si.[11]

Unfortunately, this discussion remains qualitative, since due to the lack of experimental data the optical-phonon branches of ZnSe and their eigenvectors are not known with the high accuracy required for the present work. In closing, we note that, in principle, the isotope disorder and anharmonic contributions to the self-energy have to be taken into account simultaneously, as they might well be of similar size.[37,38] For example, isotope-disorder-induced scattering can open additional anharmonic decay channels and vice versa. Therefore, the independent treatment of these two effects could well yield results that do not agree with the observation. Although we have checked that the mere addition of the anharmonic contribution (0.4 cm^{-1} FWHM) to the isotope-disorder-induced line-width in the line shape expression [Eq. (5)] does not alter the qualitative conclusions drawn for the TO(Γ) phonon, at present it is hard to predict the results of a simultaneous treatment using the precise phonon dispersion and the eigenvectors of the optical branches in ZnSe.

B. Anharmonicity and plasmon-phonon coupling

The phonon linewidth in a perfect crystal, i.e., in the absence of isotope disorder and/or free carriers induced by dopants, is determined by the anharmonic interaction. In most cases it is sufficient to take into account third-order coefficients V_3 of the lattice potential vs. atomic displacement.[39] In order to check whether the observed differences of the TO(Γ) and LO(Γ) linewidths of the isotopically pure samples, i.e., ~ 0.4 cm^{-1} and ~ 1.5 cm^{-1}, respectively, are consistent with the anharmonic decay scenario, we make the following approximations: since the third-order coefficients V_3 are not available for ZnSe, we assume them to be constant, i.e., independent of the frequency within the range relevant here. Under this assumption, the lifetime of the phonons at low temperatures should be proportional to the two-phonon density of states (obtained with the **q**-conservation constraint), i.e., $\Gamma_{anh}(\omega)=\mathcal{V}_{eff}\rho_2(\omega)$ (FWHM), where we have used an effective interaction coefficient $\mathcal{V}_{eff}$.[8] Identifying the lifetime with the imaginary part of the self-energy, we can calculate the corresponding real part by Kramers-Kronig transformation. The line shape can be then calculated with an expression similar to Eq. (5). The results are presented in Fig. 10, where the solid line shows the negative real part $-\Delta_{anh}(\omega)$, while the dashed line shows the imaginary part $\Gamma_{anh}(\omega)$ of the anharmonic self-energy. The phonon spectra (bottom part of Fig. 10) were obtained using $\omega_j(\mathbf{q}=0)=209$ cm^{-1} and 258 cm^{-1} for the

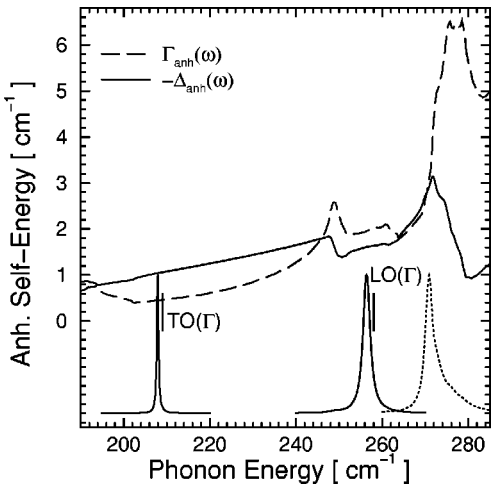

FIG. 10. The dashed line shows the imaginary part of the anharmonic self-energy, assumed to be proportional to the two-phonon density of states [$\Gamma(\omega)=\mathcal{V}_{eff}\rho_2(\omega)$, FWHM]. The two-phonon density of states of $^{nat}Zn^{nat}Se$ was calculated using the RIM and the parameters of Ref. 33 and normalized to a value of 36. The solid line represents the real part of the anharmonic self-energy (with its sign reversed). The corresponding simulated TO and LO Raman spectra are shown below these lines as solid lines; the dotted line shows an asymmetric LO line, which is explained in the text.

TO and LO phonon, respectively. The bare frequencies are shown by the vertical lines. We have used $\mathcal{V}_{eff}=22$ cm^{-2}, since this value yields a linewidth for the TO(Γ) phonon of about 0.4 cm^{-1}. We observe that the two phonons have linewidths which differ by a factor of ~ 4, so that this simple approximation qualitatively accounts for the experimental results.

In principle, the anharmonic decay could also be responsible for the asymmetric and broad LO(Γ) lines observed for $^{64}Zn^{76}Se$ and $^{64}Zn^{80}Se$, which have the smallest reduced masses and, therefore, the largest unrenormalized phonon frequencies. We notice that there is a steep increase in the calculated $\Gamma_{anh}(\omega)$ around 270 cm^{-1}. Therefore, we obtain an asymmetric line shape when using $\omega_j(\mathbf{q}=0)=274$ cm^{-1} as the bare frequency. The resulting spectrum is represented by the dotted line in Fig. 10. In reality, the steep increase of $\Gamma_{anh}(\omega)$ might occur at lower frequencies, since the phonon dispersion was obtained from fits of a RIM to the neutron data.[33] The fact that the linewidths of samples with the largest unrenormalized frequencies are asymmetric is consistent with this simulation. However, isotope substitution affects the BZ center mode energies $\omega_j(\mathbf{q}=0)$ according to their reduced mass dependence and those contributing to the two-phonon density of states $\rho_2(\omega)$ according to their respective eigenvectors, which are not known precisely. If we asssumed strongly mixed, e.g., reduced-mass-like, modes to contribute to $\rho_2(\omega)$ in this energy range, we would have to expect all other samples to be equally asymmetric, which clearly is not the case. The assumption of purely Se-like or Zn-like oscillators contributing to $\rho_2(\omega)$ cannot explain the trends either (see Table I), so that the observations cannot be reconciled with an anharmonic decay process in a straightforward manner.

Another possible reason for the shoulders in the LO spectra of the $^{64}Zn^{76}Se$ and $^{64}Zn^{80}Se$ sample is their coupling to

the longitudinal collective plasmon excitation, associated with free carriers in the material.[40] The plasmon-phonon interaction becomes important when the plasma frequency ω_p approaches the frequency of LO(Γ).[41] An anticrossing of the two excitations occurs as a function of the carrier density, so that for small densities the LO phonon-like mode is repelled to larger energies. For ZnSe, we calculate that a carrier density of 1×10^{16} cm^{-1} would result in an upward shift of the LO phonon of about 2 cm^{-1}. These carrier densities may well occur in some of our samples, since the starting materials, i.e., the isotopically pure elements, are not chemically pure and, due to the small amounts of available material, the usual purifying techniques (e.g., zone melting) could not be applied. If we assumed that such a carrier density occurs in the ^{64}Zn^{76}Se and ^{64}Zn^{80}Se sample, and that it is inhomogeneously distributed over the sample (an assumption necessary in order to explain the observed spectra, i.e., a distribution of peaks), we could explain the shoulders in the corresponding LO(Γ) spectra in Fig. 4. However, there is no particular reason why only these two samples should be affected, so that hitherto the origin of the LO(Γ) shoulders is not fully understood.

C. Mass and temperature dependence of the fundamental gap

The mean-square vibrational amplitude $\langle u^2\rangle$ of an atom depends on the phonon frequencies and the eigenvectors, the atomic masses (at low temperatures), as well as the temperature (at high T). Isotope substitution results in slightly different vibrational amplitudes (especially at low T) and phonon frequencies and is roughly equivalent to changing the temperature. The mass dependence of $\langle u^2\rangle$ becomes vanishingly small at temperatures on the order or higher than the Debye temperature. Changes in either the isotope masses or temperature thus lead to changes in the band gap via the electron-phonon interaction, even at zero temperature in the case of mass changes. In general, the renormalization of the band gap and its temperature dependence result from a complicated interplay of (i) first- and second-order electron-phonon interactions that contribute to the energy of the conduction and valence bands, (ii) changes due to thermal or isotopic lattice expansion, and (iii) changes in the phonon occupation numbers. A method to calculate the temperature dependence of semiconductor band gaps based on local empirical pseudopotentials and lattice-dynamical models was developed in a series of articles.[42] This work has subsequently been extended to calculations of the band gap dependence on the isotope mass.[13,16]

The main ideas and results have been summarized in Refs. 14, 15, and 18 and a simple approximation of the full calculation was presented and applied to CuCl, CuBr, and CdS. In this model, we have neglected the contribution of the isotopic lattice expansion to the band gap renormalization and have approximated the lattice dynamics of CuCl by two harmonic oscillators (modified Einstein model). One oscillator represents an average acoustic phonon whereas a second oscillator represents an average optic phonon. Due to the large mass difference between Cu and Cl, it is reasonable to associate the acoustic and optic oscillator with a pure copper and a pure chlorine vibration, respectively.

In contrast, zinc and selenium have rather comparable masses. Therefore, we employ a different approximation for the lattice dynamics of ZnSe: One oscillator at 100 cm^{-1} represents an average acoustic phonon having a total-mass-like dependence of its frequency ($\omega_{\rm tot}\sim m_{\rm tot}^{-1/2}; m_{\rm tot}=m_{\rm Se}+m_{\rm Zn}$) a second oscillator at 220 cm^{-1} represents an average optic phonon having a reduced-mass-like dependence of its frequency ($\omega_\mu\sim\mu^{-1/2}; \mu^{-1}=m_{\rm Se}^{-1}+m_{\rm Zn}^{-1}$). These frequencies correspond to the mean frequency of the acoustic and optic band, respectively, of the total DOS. The results obtained when associating the acoustic oscillator with pure Se vibration and the optic oscillator with a pure Zn vibration will be discussed below. Within this approximation, we describe the total mass and temperature dependence of the fundamental gap by[15,18]

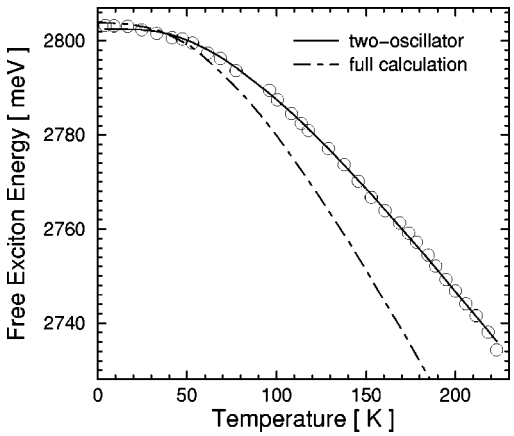

FIG. 11. Temperature dependence of the free-exciton ($\equiv$band gap) energy of ZnSe. The experimental data (open circles) were taken from Ref. 25. The solid line represents our fit of a two-oscillator model to the data. The dashed-dotted line shows the results of the detailed calculation of the temperature dependence of the band gap in ZnSe as discussed in Ref. 13.

$$E_0(T,m_{\rm Se},m_{\rm Zn})=E_0+\frac{A_{\rm tot}}{\omega_{\rm tot}m_{\rm tot}}[n(\omega_{\rm tot},T)+\tfrac{1}{2}]+\frac{A_\mu}{\omega_\mu\mu}[n(\omega_\mu,T)+\tfrac{1}{2}], \quad (6)$$

where E_0, $A_{\rm tot}$, and A_μ can be determined from a fit to the measured temperature dependence of the gap. Taking into account the proportionality of the oscillator frequency to the inverse square root of its mass, we find the gap shifts due to the isotope substitution of either Se or Zn at zero temperature to be

$$\frac{\partial E_0(T=0,m_{\rm tot},\mu)}{\partial m_{\rm Se/Zn}}=-\frac{1}{4}\left(\frac{A_{\rm tot}}{\omega_{\rm tot}m_{\rm tot}^2}+\frac{A_\mu}{\omega_\mu m_{\rm Se/Zn}^2}\right). \quad (7)$$

We represent the experimentally determined temperature dependence of the free exciton in natural ZnSe (from Ref. 25) by circles in Fig. 11. The solid line shows the fit of Eq. (6), while the dashed-dotted line are the predictions from Ref. 13. The two-oscillator model describes the observed temperature dependence quite well. From the fit of Eq. (6) and using Eq. (7) we obtain $\partial E_0/\partial m_{\rm Se}=182(50)\,\mu$eV/amu and $\partial E_0/\partial m_{\rm Zn}=237(50)\,\mu$eV/amu for the mass dependence of the fundamental gap at zero temperature. This is in good

agreement with our experimental data of 216(30) μeV/amu and 214(30) μeV/amu for selenium and zinc substitution, respectively. We note that the coefficients determined by means of isotope substitution are more precise than those inferred from the temperature dependence on the basis of our two-oscillator model. The full calculation presented in Ref. 13, which comprises the contributions from the isotopic lattice expansion and first- and second-order electron-phonon interactions, predicts 300 μeV/amu and 310 μeV/amu for selenium and zinc substitution, respectively. These values are a factor of 1.5 larger than the measured ones. Correspondingly, the calculated temperature dependence of the gap (dashed-dotted line in Fig. 11) is also 50% larger than the measured one.

The size of the contribution arising from the isotopic lattice expansion can be estimated using Eq. (9) of Ref. 13 $[(\partial E_0/\partial m_\kappa)_{TE} = -3B(\partial E_0/\partial p)_m(\partial \ln a_0/\partial m_\kappa)_p$, where a_0 denotes the lattice constant, *TE* stands for thermal expansion, and *m* and *p* label constant mass and constant pressure, respectively]. The bulk modulus *B* of ZnSe is 64.7 GPa at 4 K and is essentially constant throughout the temperature range of interest here (62.4 GPa at room temperature).[43] The pressure dependence of the direct gap is also practically independent of temperature $[(\partial E_0/\partial p)_m = 75(3)$ meV/GPa$]$.[43] The relative change of the lattice constant with isotopic composition was calculated in Refs. 13 and 19. These results differ somewhat: $(\partial \ln a_0/\partial m_{\mathrm{Zn}})_p = -7.95\times10^{-6}$ amu^{-1} and $(\partial \ln a_0/\partial m_{\mathrm{Se}})_p = -2.70\times10^{-6}$ amu^{-1} in Ref. 13, versus $(\partial \ln a_0/\partial m_{\mathrm{Zn}})_p = -4.80\times10^{-6}$ amu^{-1} and $(\partial \ln a_0/\partial m_{\mathrm{Se}})_p = -3.43\times10^{-6}$ amu^{-1}, in Ref. 19. Using these values one finds $(\partial E_0/\partial m_{\mathrm{Zn}})_{\mathrm{TE}} = 116$ μeV/amu and $(\partial E_0/\partial m_{\mathrm{Se}})_{\mathrm{TE}} = 39$ ∂eV/amu from the calculations based on empirical lattice-dynamical models[13] and 70 μeV/amu and 50 μeV/amu for the respective values from *ab initio* calculations.[19] Thus, the correction of the band gap arising from the dependence of the lattice constant on the isotope masses amounts to less than 30% of the total at low temperatures. Therefore, the omission of this contribution in the two-oscillator model might affect the coefficients determined from the fit but does not render the model inapplicable.

It should be mentioned that two-oscillators have been used earlier to approximate the observed temperature dependence of the band gap in group-IV semiconductors[44] and that it was found that the best fit yielded the average frequencies of the acoustic- and optic-phonon branches. Manoogian and Wooley[45] have shown that the well known Varshni[46] formula is equivalent to second-order expansion of a Bose-Einstein population factor valid at high temperatures. Viña, Logothetidis, and Cardona used a single average oscillator (phonon) to describe the temperature dependence of interband critical points of a number of group-IV and -III-V semiconductors,[47] a model that is often sufficient in view of the experimental uncertainties.

We note that there are two main alternatives for the mass dependence of the two oscillators used in the model: (i) The assumption of a total-mass-like oscillator at 100 cm^{-1} ($m_{\mathrm{tot}} = m_{\mathrm{Se}} + m_{\mathrm{Zn}}$) and one reduced-mass-like oscillator at 220 cm^{-1} is in part supported by *ab initio* calculations that find that the Se and Zn eigenvectors of the TA and TO branches in ZnSe have values similar to those at the Γ point for all wave vectors.[48] (ii) The other obvious assumption would be that of an acoustic Se-like oscillator and an optic Zn-like harmonic oscillator. This in part motivated by the fact that in the acoustic energy range $\rho_{\mathrm{Se}}(\omega)$ contributes $\sim$62% to the total DOS. In contrast, the optic energy range is dominated by $\rho_{\mathrm{Zn}}(\omega)$ with $\sim$60%. Furthermore, the LA and LO phonons around the *X* point are characterized by independent Se and Zn displacements, respectively.[33] In this case, we obtain $\partial E_0/\partial m_{\mathrm{Se}} = 116(50)$ μeV/amu and $\partial E_0/\partial m_{\mathrm{Zn}} = 317(50)$ μeV/amu for the mass dependence of the fundamental gap at zero temperature. These values are not in as good an agreement with the experimental findings as those obtained from the mixed Se and Zn total and reduced-mass-like harmonic oscillators assumption. However, based on these results we cannot judge which of the two considerations is more realistic since the errors in the fit to the temperature dependence are rather large. We emphasize again that the approximation of the electron-phonon interaction strengths by the two constants A_{tot} and A_μ may introduce considerable errors. In a full calculation, the *A*'s would differ for different phonons and electron bands [compare Fig. 3 in Ref. 13 and Eq. (13) in Ref. 13] so that the individual phonon contributions would be weighted differently, an effect that cannot be predicted easily.

In summary, we have shown that the two-oscillator model is able to describe the temperature dependence of the band gap of ZnSe and yields values for its dependence on isotope mass that are in good agreement with the experimentally determined values. Obviously, this model can achieve a more accurate (quantitative) parametrization of the observed temperature dependences than earlier formulas proposed in Refs. 46 and 47 as we employ more parameters. In addition, it also improves the parametrization of those band-gap temperature dependences that exhibit pronounced kinks and/or increases with increasing temperature.[15]

V. SUMMARY AND CONCLUSIONS

Isotope substitution provides means of changing the energies of vibrational excitations in a crystal. Therefore, it can be employed to study renormalization effects in intrinsic semiconductors such as the phonon-phonon interaction (isotope disorder or anharmonic scattering) and the band-gap renormalization due to the electron-phonon interaction. The anharmonic phonon-phonon and electron-phonon interactions depend mostly on the masses of the isotopes used. While it is clear that the magnitude of these renormalization effects decreases with increasing mass and, correspondingly, increases with increasing temperature, the actual size (and sign in the case of the electron-phonon interaction) cannot be predicted easily. The isotope-disorder-induced effects depend on the mass variance of the isotopes on the respective sublattice.

In this publication, we have dealt with a number of these effects that we have identified in ZnSe. The lifetime of the transverse optic phonon at the zone center at low temperatures was found to depend strongly on the isotopic purity of the material, i.e., strong isotope disorder-induced scattering occurs due to a large density of final states in this energy range, which stems from the flat TO-phonon branches. The TO(Γ) frequency is also affected by the isotope disorder

contributions to the self-energy, and is (slightly) repelled towards lower energies, away from the range of a high one-phonon density of states. The TO(Γ)-phonon energies of the nominally isotopically pure samples obey the reduced-mass rule expected in a zinc-blende compound [$\omega(\Gamma) \sim \mu^{-1/2}$]. For the LO($\Gamma$) phonons, we find neither a significant isotope disorder contribution to their energy nor can we discern a disorder-induced broadening from other potential contributions like plasmon-phonon coupling and anharmonic interactions to the linewidth. We realize that a better knowledge of the lattice dynamics of ZnSe might be required to enable a fully quantitative line shape analysis.

We have used *isotope substitution* to tune the phonon frequencies in our samples and to measure the changes in the band gap as observed in the luminescence spectra at 2 K. For cation as well as anion substitution, we found the normal[1,13,18] gap *increases* with *increasing* mass. This (usual) behavior has been observed so far in elemental and compound semiconductors. We have treated the band-gap renormalization as being caused by two effective phonon oscillators, one at high (optic) and one at low (acoustic) frequencies, that approximate the lattice dynamics of ZnSe. This model leads to simple expressions for the mass and temperature dependence of the band gap. A fit of the temperature dependence[25] yielded values that are in reasonable agreement with the experimentally determined dependences of the band gap on the isotope masses.

ACKNOWLEDGMENTS

We are indebted to J. Kuhl for a critical reading of the manuscript. A.G. gratefully acknowledges stimulating discussions with V. Belitsky, A. Cantarero, and T. Strohm. We are grateful to A. Schmeding for the isotope analysis and O. Buresch for the chemical analysis of our samples.

*Present address: Department of Electrical Engineering, The University of British Columbia, Vancouver, B.C., Canada V6T 1Z4.

[1] M. Cardona, in *Festkörperprobleme/Advances in Solid State Physics*, edited by R. Helbig (Vieweg, Braunschweig/Wiesbaden, 1994), Vol. 34, p. 35.
[2] A. K. Ramdas, Solid State Commun. **96**, 111 (1995).
[3] E. E. Haller, J. Appl. Phys. **77**, 2857 (1995).
[4] T. Ruf, H. D. Fuchs, and M. Cardona, Phys. Bl. **52**, 1115 (1996).
[5] J. M. Zhang, T. Ruf, A. Göbel, A. Debernardi, R. Lauck, and M. Cardona, in *The Physics of Semiconductors*, edited by M. Scheffler and R. Zimmermann (World Scientific, Singapore, 1996), p. 201.
[6] J. M. Zhang, T. Ruf, M. Cardona, O. Ambacher, M. Stutzmann, J.-M. Wagner, and F. Bechstedt, Phys. Rev. B **56**, 14 399 (1997).
[7] F. Widulle, T. Ruf, O. Buresch, A. Debernardi, and M. Cardona, in *The Physics of Semiconductors* (World Scientific, Singapore, in press).
[8] A. Göbel, T. Ruf, M. Cardona, C. T. Lin, and J. C. Merle, Phys. Rev. Lett. **77**, 2591 (1996); A. Göbel, T. Ruf, C. T. Lin, M. Cardona, J. C. Merle, and M. Joucla, Phys. Rev. B **56**, 210 (1997).
[9] A. Göbel, D. T. Wang, M. Cardona, L. Pintschovius, W. Reichardt, J. Kulda, N. M. Pyka, K. Itoh, and E. E. Haller, Phys. Rev. B **58**, 10 510 (1998).
[10] J. M. Zhang, M. Giehler, A. Göbel, T. Ruf, M. Cardona, E. E. Haller, and K. Itoh, Phys. Rev. B **57**, 1348 (1998).
[11] F. Widulle, T. Ruf, A. Göbel, I. Silier, E. Schönherr, M. Cardona, J. Camacho, A. Cantarero, and W. Kriegseis, in *Proceedings of the 9th International Conference on Phonon Scattering in Condensed Matter* [Physica B (to be published)].
[12] D. T. Wang, A. Göbel, J. Zegenhagen, and M. Cardona, Phys. Rev. B **56**, 13 167 (1997).
[13] N. Garro, A. Cantarero, M. Cardona, A. Göbel, T. Ruf, and K. Eberl, Phys. Rev. B **54**, 4732 (1996).
[14] N. Garro, A. Cantarero, M. Cardona, T. Ruf, A. Göbel, C. T. Lin, K. Reimann, S. Rübenacke, and M. Steube, Solid State Commun. **98**, 27 (1996).
[15] A. Göbel, T. Ruf, M. Cardona, C. T. Lin, J. Wrzesinski, M. Steube, K. Reimann, J.-C. Merle, and M. Joucla, Phys. Rev. B **57**, 15 183 (1998).
[16] S. Zollner, M. Cardona, and S. Gopalan, Phys. Rev. B **45**, 3376 (1992); C. Parks, A. K. Ramdas, S. Rodriguez, K. M. Itoh, and E. E. Haller, *ibid.* **49**, 14 244 (1994).
[17] D. Rönnow, L. F. Lastras-Martínez, and M. Cardona, Eur. Phys. J. B **5**, 29 (1998).
[18] J. M. Zhang, T. Ruf, R. Lauck, and M. Cardona, Phys. Rev. B **57**, 9716 (1998).
[19] A. Debernardi and M. Cardona, Phys. Rev. B **54**, 11 305 (1996).
[20] R. C. Buschert, A. E. Merlini, S. Pace, S. Rodriguez, and M. H. Grimsditch, Phys. Rev. B **38**, 5219 (1988).
[21] A. Kazimirov, J. Zegenhagen, and M. Cardona, Science **282**, 930 (1998).
[22] M. Asen-Palmer, K. Bartkowski, E. Gmelin, M. Cardona, A. P. Zhernov, A. V. Inyushkin, A. Taldenkov, V. I. Ozhogin, K. Itoh, and E. E. Haller, Phys. Rev. B **56**, 9431 (1997); W. S. Capinski, H. J. Maris, E. Bauser, I. Silier, M. Asen-Palmer, T. Ruf, M. Cardona, and E. Gmelin, Appl. Phys. Lett. **71**, 2109 (1997).
[23] W. E. Bron, J. Kuhl, and B. K. Rhee, Phys. Rev. B **34**, 6961 (1986).
[24] S. Anand, P. Verma, K. P. Jain, and S. C. Abbi, Physica B **226**, 331 (1996).
[25] Y. Shirakawa and H. Kukimoto, J. Appl. Phys. **51**, 2014 (1980).
[26] Commission on Atomic Weights and Isotopic Abundances Report for the International Union of Pure and Applied Chemistry, in *Isotopic Compositions of the Elements 1989* [Pure and Applied Chemistry **70**, 217 (1998)]; as cited in *Web Elements 2.0:* http://www.shef.ac.uk/chemistry/web-elements/
[27] S.-I. Tamura, Phys. Rev. B **30**, 849 (1984).
[28] R. Lauck and E. Schönherr, J. Cryst. Growth **197**, (1998).
[29] D. W. Posener, Aust. J. Phys. **12**, 184 (1959).
[30] J. L. Merz, H. Kukimoto, K. Nassau, and J. W. Shiever, Phys. Rev. B **6**, 545 (1972).
[31] S.-I. Tamura, Phys. Rev. B **27**, 858 (1983); **30**, 849 (1984); H. J. Maris, *ibid.* **41**, 9736 (1990).
[32] K. Kunc and O. H. Nielsen, Comput. Phys. Commun. **16**, 181 (1979).
[33] D. N. Talwar, M. Vandevyver, K. Kunc, and M. Zigone, Phys. Rev. B **24**, 741 (1981).
[34] B. Hennion, F. Moussa, G. Pepy, and K. Kunc, Phys. Lett. A **36**, 376 (1971).

[35] M. S. Kushwaha and S. S. Kushwaha, J. Phys. Chem. Solids **41**, 489 (1980).
[36] A. Dal Corso, S. Baroni, R. Resta, and S. de Gironcoli, Phys. Rev. B **47**, 3588 (1993).
[37] A. A. Maradudin and S. Califano, Phys. Rev. B **48**, 12 628 (1993).
[38] A. Göbel, J. M. Zhang, T. Ruf, R. Lauck, and M. Cardona, in *The Physics of Semiconductors* (World Scientific, Singapore, in press).
[39] A. Debernardi, Phys. Rev. B **57**, 12 847 (1998).
[40] G. Abstreiter, M. Cardona, and A. Pinczuk, *Light Scattering by Free Carrier Excitations in Semiconductors*, in Topics in Applied Physics: Light Scattering in Solids IV, edited by M. Cardona and G. Güntherodt (Springer, Heidelberg, 1984).
[41] H. R. Chandrasekhar and A. K. Ramdas, Phys. Rev. B **21**, 1511 (1980).
[42] P. B. Allen and M. Cardona, Phys. Rev. B **27**, 4760 (1983); P. Lautenschlager, P. B. Allen, and M. Cardona, *ibid.* **31**, 2163 (1985); S. Gopalan, P. Lautenschlager, and M. Cardona, *ibid.* **35**, 5577 (1987); P. B. Allen, Philos. Mag. B **70**, 527 (1994).
[43] *Physics of Group II-VI and I-VII Compounds*, edited by O. Madelung, M. Schulz, and H. Weiss, Landolt-Börnstein, New Series, Group III, Vol. 22, Pt. a (Springer, Berlin, 1987).
[44] A. Manoogian and A. Leclerc, Can. J. Phys. **57**, 1766 (1979).
[45] A. Manoogian and J. C. Woolley, Can. J. Phys. **62**, 285 (1984).
[46] Y. P. Varshni, Physica (Amsterdam) **34**, 149 (1967).
[47] L. Viña, S. Logothetidis, and M. Cardona, Phys. Rev. B **30**, 1979 (1984).
[48] A. Debernardi (private communication).